

Cyclic Flow Patterns in Human Coronary Arteries

S Corney¹, PR Johnston², D Kilpatrick¹

¹School of Medicine, University of Tasmania, Australia

²School of Science, Griffith University, Australia

Abstract

Biplane digital coronary angiograms, as routinely performed in angiography, are used to construct a three-dimensional model of the coronary arteries. This model is used to solve the fluid flow equations throughout the cardiac cycle.

The spatial position of the centreline of the artery is determined in three dimensions by detecting the ridge line in the two images and using the rotation angles embedded in the DICOM format. Combining this with the arterial radii taken from the images allows a model of the surface of the artery to be built. This model is then discretised and a mesh constructed, both on its surface and within, which allows for a computational fluid dynamics package to solve the Navier-Stokes equations and provide detailed flow patterns, including wall shear stress.

In a series of 4 patients the right coronary artery has been reconstructed throughout the cardiac cycle, and flows have been calculated for a typical pressure gradient at each step. The flow shows a wide variation of shear stresses with variations being due to both altered velocities as well as the altered configuration of the coronary due to systolic movement. The techniques of reconstruction appear robust, as can be shown by introduction of random noise in the model.

1. Introduction

There has been unresolved debate about the haemodynamic patterns causing the development of atheroma. Asakura and Karino [1] have measured flows in a reconstructed coronary artery by fixing the artery tree to a frame, rendering the walls transparent and observing particle paths. These works showed remodelling to be a function of flow. Observations from the pathologic study on young persons dying of accidents have shown a predilection of atheroma in coronary arteries to be in certain sites [2].

We have developed a simple technique for processing digital angiograms into initially a three-dimensional outline of the wall of the coronary artery and subsequent discretisation of this artery and application of fluid dynamics computations to produce shear stress.

2. Methods

This study was approved by the University of Tasmania and the Royal Hobart Hospital Human ethics committee.

Angiography was performed on patients using routine techniques. A Siemens bicor digital angiographic unit gave time-aligned images in two simultaneous planes. The planes were not necessarily orthogonal but chosen because they occur routinely in clinical angiography. The DICOM format gives the angulation in two planes as part of the digital output. These angles are used in the computation. The digital images are read from the DICOM CD into a JPEG viewing program. Images are selected from a paired set which adequately define side branches. It is possible to use non-simultaneous images using the recorded ECG for alignment.

2.1. Image processing

Several different techniques exist for creating three-dimensional models of coronary arteries (or other internal features of the body). Most of these methods rely on reconstruction of the chosen feature from two non-planar angiographic images [3, 4, 5, 6], although some use tomographic techniques instead of, or in conjunction with, angiography (see for example [7]). The reconstruction method detailed here is based on the technique developed by Metz and Fencil [3].

In order to carry out the reconstruction algorithm, which will be given below, it is necessary to identify the centreline and edge of the chosen artery. These processes are done separately, resulting in two images, one containing the edge detection, and one the centrelines, which are then recombined (see figure 1). The image is first smoothed using standard Gaussian smoothing. The edge detection is carried out using Canny edge-detection [8] on a 3×3 kernel, followed by two-level thresholding and edge synthesis.

The centreline is detected using the ridge detection algorithm developed by Lopez [9] based on the multilocal level curve curvature. This method is a multilocal crease detector method which suffers less discontinuities than more common crease detectors. In order to extract good creases a threshold value [9] for the multilocal level curve curvature $|\kappa|$ of 0.25 is chosen.

Finally a one-pass thinning algorithm [10] is applied to

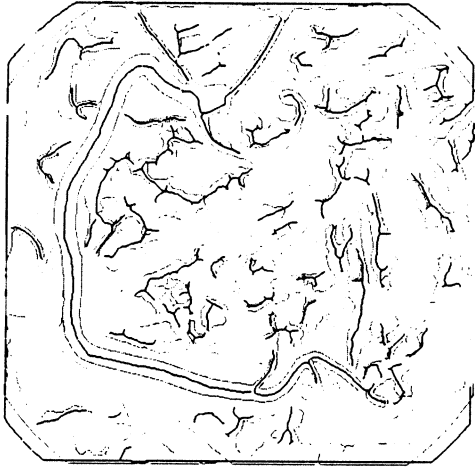


Figure 1. A discrete image, showing the edges (grey) and centreline (black) of the RCA

both images and any edges/centrelines are deleted that are less than 60 pixels long. The two images are then added together on a white background so that the centreline is black and edgelines are grey. The result is shown in figure 1.

Once both images have been discretised the beginning of the desired artery is selected by a user in each image. At this stage only the main branch of the RCA will be considered, and so any branching is ignored. Once this initial point is defined the artery can be automatically tracked, and the radius at each point determined. In order to reconstruct the artery in three dimensions the two angles which define the transformation between the two images must be known. This information is embedded in the DICOM format of the CD and thus can be recovered and used. An approximation of the physical distance between the two image planes is also required.

Given these angles it is possible to determine the transformation which takes a point from the first image into the second image, using an adaptation of the Metz-Fencil technique [3]. The Metz-Fencil technique uses points on each image which are known to coincide (fiducial points) to determine the rotation parameters. Here the rotation parameters are already known, and so it is possible to select a point on one image and determine a line containing the corresponding point on the other image. Due to the deficiency in information from a two-dimensional image it is not possible to calculate the corresponding point exactly, only the line upon which it must lie, however the intersection between this line and the chosen artery is the desired point.

From [3], it can be shown that the line of correspondence in the second image has the equation

$$\xi' = M\eta' + C, \quad (1)$$

where

$$M = -\frac{\xi(r_{23}t_y - r_{22}t_x) + \eta(r_{21}t_x - r_{23}t_z) + (r_{22}t_z - r_{21}t_y)}{\xi(r_{13}t_y - r_{12}t_x) + \eta(r_{11}t_x - r_{13}t_z) + (r_{12}t_z - r_{11}t_y)}, \quad (2)$$

$$C = -\frac{\xi(r_{33}t_y - r_{32}t_x) + \eta(r_{31}t_x - r_{33}t_z) + (r_{32}t_z - r_{31}t_y)}{\xi(r_{13}t_y - r_{12}t_x) + \eta(r_{11}t_x - r_{13}t_z) + (r_{12}t_z - r_{11}t_y)},$$

where (ξ, η) and (ξ', η') are the coordinates of the point in the two images, $R = (r_{ij})$ is the rotation matrix transforming the first image plane into the second, and (t_x, t_y, t_z) is the translation vector between the two image planes. Thus, once (ξ, η) is selected in the first image, it is possible to determine a line, whose intersection with the artery in the second image provides the corresponding point (ξ', η') . This allows corresponding points along the length of the artery to be determined, giving an accurate reconstruction in three dimensions.

If the two imaging guns of the angiogram are isocentric then the above method should yield a unique (x, y, z) for every point along the artery. However in practice they are often slightly off-centre [5], and thus some error correction is needed. Fortunately the presence of fiducial points in the images provide excellent markers for error correction, as their position can be accurately determined in both planes. The correction is carried out by minimising the adjustments needed to the coefficients M and C to ensure that any identified fiducial points correspond in both images.

2.2. Mesh construction

As detailed above, biplane angiograms give the centre line of the artery as well as two radii at each point. This information is now used to create a mesh suitable for computational fluid dynamical modelling of the blood flow in the artery. The first step is to re-orient the centre line so that the origin is at the proximal end of the artery and the positive z direction points into the artery. The next step is to create a mesh across the proximal end of the artery and then extrude this along the centre line, changing the radii as necessary.

Before any re-orientation is performed, the centre line is interpolated up to about 400 points using a cubic spline so that a smooth artery is achieved. The radii are also interpolated, but in this case linear interpolation is used due to the localised changes in radius along the artery.

2.2.1 Re-orientating the Centre Line

The proximal end of the centre line is set to the origin via a simple translation of all points defining the centre line.

The entire centre line is rotated about the new origin so that the entrance to the flow domain lies in the $x - y$ plane. The idea here is to rotate the centre line such that the first interpolated point along the centre line, away from the origin, lies along the z -axis. This is achieved by finding the polar and azimuthal angles $\phi = \arccos z_2$ and $\theta = \arctan \frac{y_2}{x_2}$ of the point (x_2, y_2, z_2) . This point is then

rotated about the z -axis clockwise through the angle θ , then about the y -axis anticlockwise through the angle ϕ . Each point along the centre line of the artery also undergoes the same transformation.

At the same time, the artery is rotated around the z -axis so that the lateral plane coincides with the $x - z$ plane. Hence the lateral plane radius specified in the data file is the length of the semi-major axis in the x direction.

2.2.2 Meshing the Entrance Plane

A two-dimensional mesh is created for the entrance plane and then extruded along the interpolated centre line.

For simplicity, the entrance mesh is based on the standard technique for meshing a circle of unit radius. This circle is then scaled in the x and y directions to form an ellipse of the appropriate size.

To mesh the unit circle, consider a circle centred on the origin. A square a of side length $2a$ is introduced at the origin, where usually $0.4 \leq a \leq 0.6$. Straight lines are then constructed from the corners of the square out to the circle, which by construction bisect the circle in each quadrant. A suitable mesh can then be constructed by meshing each of the five quadrilaterals obtained.

2.2.3 Extruding the Mesh

The final step in creating the three-dimensional mesh is to extrude the entrance mesh along the interpolated centre line. Copies of the entrance mesh are moved along the interpolated centre line at equal increments. Straight lines joining equivalent nodes in adjacent cross-sectional meshes are created to form an approximation to the artery consisting of brick elements.

The normal direction to the plane of the mesh is taken as parallel to the vector joining the previous and subsequent points along the centre line. The technique chosen for creating copies of the entrance mesh is to find the change in the normal direction from one cross section to the next. This is achieved using the concept of finite rotations [11]. The advantage of this approach is that the angles through which rotations are performed are small and, hence, there is a reduced possibility of unnecessary changes in orientation from one cross section to the next. Figure 2 shows a typical three-dimensional mesh constructed from data obtained directly from two biplane angiograms. The inset to this figure shows a close-up of the entrance mesh.

3. Results

Atheroma in human coronary arteries has a predilection for certain sites [2]. Of the factors which are thought to contribute to atheroma formation, the patterns of flow and the structure of the wall are the only two which might relate to the position of the atheroma. The conditions of blood

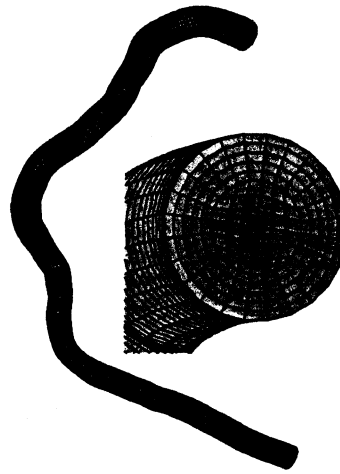


Figure 2. Example of a mesh of the right coronary artery. Inset: close up view of the entrance plane.

flow at the arterial wall are bound by the rate of change of velocity from the wall into the stream, and the wall shear stress. Both high and low shear stress have been proposed to cause arterial damage.

In a series of four patients the right coronary artery has been reconstructed every $0.08s$ throughout the cardiac cycle, leading to approximately 12 distinct reconstructed arteries for each patient. The flow of blood through each of these reconstructed arteries was calculated using the computational fluid dynamics package CFD-ACE. This package solved the Navier-Stokes equations providing detailed flow patterns inside the arteries, including the wall shear stress. Boundary conditions included a constant flow perpendicular to the inlet, and zero pressure at the outlet. During diastole the inlet velocity was set to $0.05ms^{-1}$, whilst during systole the velocity was $0.2ms^{-1}$.

In the diastolic phase the blood flow through the coronary arteries is low, and thus wall shear stress is low throughout the artery, and only slowly changing, however in the systolic phase the flow increases, and significant changes are seen in the wall shear stress both spatially and temporally. In figure 3 the RCA of a patient is shown over a period of $0.4s$ from the start of systole. Figure 4 shows a close-up of the bottom section of the last two images. In this figure the changes, both in the conformation of the artery, and the resulting change in the wall shear stress pattern, are clearly visible.

Similar results are obtained for each of the four patient's studied, although the degree to which the patterns changed was very much dependent on the individual patients geometry.

Due to pixel resolution from the DICOM images and unavoidable inaccuracy in the reconstruction algorithm

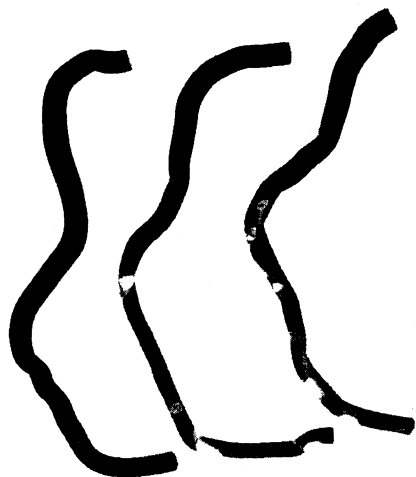


Figure 3. Wall shear stress in the right coronary artery. The left image is at systole, the centre 0.24s later and the right 0.4s after systole. The shear stress ranges from $0N/m^2$ (black) to $14.0N/m^2$ (white).



Figure 4. A close-up view of the two later images from figure 3. The two images are only 0.16s apart, but show marked changes in the patterns of wall shear stress.

robustness of the model is essential. Figure 5 shows the start of diastole for a different patient with random errors introduced to the two radii, of the order of 10% of the initial value. It can be seen that these errors introduce slight changes into the wall shear stress patterns, however the overall distribution of the wall shear stress appears robust.

References

- [1] Asakura T, Karino T. Flow patterns and spatial distribution of atherosclerotic lesions in human coronary arteries. *Circulation* 1990;66:1054.
- [2] Starry HC. Evolution and progression of atherosclerotic lesions in coronary arteries of children and young adults. *Arteriosclerosis* 1989;9:1-19.



Figure 5. Demonstration of robustness of the model; the left image is the original reconstruction of an RCA, whilst the remaining two images have a random error of up to 10% introduced into the two radii. The wall shear stress ranges from $0N/m^2$ to $9.5N/m^2$ (white).

- [3] Metz CE, Fencil LE. Determination of three-dimensional structure in biplane radiography without prior knowledge of the relationship between the two views: Theory. *Medical Physics* 1989;16:45.
- [4] Chen SJ, Carroll JD. Three-dimensional reconstruction of coronary arterial tree based on biplane angiograms. *SPIE Medical Imaging* 1996;2710.
- [5] Wahle A, Oswald H, Fleck E. 3d heart vessel reconstruction from biplane angiograms. *IEEE Computer graphics and applications* 1996;16:65.
- [6] Slager CJ, Wentzel JJ, Schuurbiens JC, Oomen JA. True 3-dimensional reconstruction of coronary arteries in patients by fusion of angiography and ivus (angus) and its quantitative validation. *Circulation* 2000;511.
- [7] Messaris G, Kolitsi Z, Badea C, Pallikarakis N. Three-dimensional localisation based on projectional and tomographic image correlation: an application for digital tomosynthesis. *Medical engineering and physics* 1999; 21:101.
- [8] Canny J. A computational approach to edge detection. *IEEE Trans Patt Anal Mach Intel* 1986;679.
- [9] Lopez A, Toledo R, Serrat J, Villanueva J. Extraction of vessel centrelines from 2d coronary angiographies. In Torre MI, Sangelin A (eds.), 8th Spanish Nat. Symp. on Patt. Recog. and Image Anal. Editions Geneve, 1999; 489.
- [10] Wu RY. A new one-pass parallel thinning algorithm for binary images. *Pattern Recog Lett* 1992;13:715.
- [11] Goldstein H. *Classical Mechanics*. Addison Wesley, 1980.

Address for correspondence:

Stuart Corney / School of Medicine / University of Tasmania
 3rd Floor / 43 Collins St / Hobart / Australia / 7000
 tel./fax: +61-3-62264807/4894
 Stuart.Corney@utas.edu.au / <http://www.cardio.utas.edu.au>